International Journal of Anatomy and Research,
Int J Anat Res 2026, Vol 14(3):9636-45. ISSN 2321-4287
DOI: https://dx.doi.org/10.16965/ijar.2026.180

Original Research Article

Effect of Selenium and Green-Synthesized Silver Nanoparticles in Embryo Culture Media on Oxidative Stress Attenuation and Developmental Competence: A Histological Study

Noor Noori.

Department of Medical Laboratory Techniques, Kut Technical Institute, Middle Technical University, Baghdad, Iraq.

ABSTRACT

Background: Developmental competence is impaired by the formation of reactive oxygen species (ROS) in in-vitro embryo culture, which results in cytological injury that can be easily detected using histological analysis. Antioxidant supplementation with nanoparticles has become an appealing approach to overcome this oxidative load.

Aims: To assess the impact of selenium nanoparticles (SeNPs) and green-synthesized silver nanoparticles (G-AgNPs), when used alone and in combination, on oxidative stress biomarkers, developmental progression, and blastocyst histoarchitecture of murine embryos in culture.

Methods: Two-cell embryos (n = 480) were randomly allocated to four groups: control (KSOM only), KSOM + 5 µg/mL SeNPs, KSOM + 2 µg/mL G-AgNPs (synthesized using an aqueous green-tea leaf extract), or KSOM containing both nanoparticles. Developmental endpoints were assessed at 48, 72, 96, and 120 h. Oxidative stress biomarkers (MDA, SOD, CAT, GPx, GSH) were measured in embryo lysates. Blastocysts were subjected to routine H&E, PAS, TUNEL, and cleaved-caspase-3 immunohistochemistry.

Results: The highest rates of blastocyst (64.7%) and hatched-blastocyst (34.5%), a 56% malondialdehyde reduction, and 1.7–2.4-fold increases in antioxidant enzyme activities were observed with combined SeNPs + G-AgNPs supplementation compared to control ($p < 0.001$). Histologically, the composite group had a well-defined inner cell mass (ICM), organized trophectoderm, minimal cytoplasmic vacuolation, and a 3.4-fold reduced TUNEL-positive nuclear count compared to controls. The correlation between lipid-peroxidation level and histological injury score was strong and positive ($r = 0.82$, $p < 0.001$).

Conclusion: Co-supplementation of SeNPs and G-AgNPs in embryo culture media maintains redox homeostasis and enhances blastocyst histoarchitecture, warranting further application in translational murine embryo production methods.

KEYWORDS: Selenium Nanoparticles, Green Silver Nanoparticles, Embryo Culture, Oxidative Stress, Blastocyst, Histology, In-Vitro Embryo Production.

Corresponding Author: Dr. Noor Noori, Department of Medical Laboratory Techniques, Kut Technical Institute, Middle Technical University, Baghdad, Iraq. **E-Mail:** noor.noori@mtu.edu.iq

Access this Article online	Journal Information
Quick Response code	**International Journal of Anatomy and Research** ISSN (E) 2321-4287 | ISSN (P) 2321-8967 **https://www.ijmhr.org/ijar.htm** **DOI-Prefix:** https://dx.doi.org/10.16965/ijar
DOI: 10.16965/ijar.2026.180	**Article Information** Received: 05 May 2026 Accepted: 25 Jul 2026 Peer Review: 15 May 2026 Published (O): 01 Sep 2026 Revised: 21 Jul 2026 Published (P): 05 Sep 2026

INTRODUCTION

The in-vitro production of embryos (IVP) has been a revolution in the field of reproductive medicine, animal breeding and conservation biology. In vitro cultured embryos are less viable, have altered gene expression and have impaired implantation capacity when compared to embryos born in vivo, although they have become a common method [1, 2]. This is mainly attributed to the increased and

persistent generation of ROS in the presence of supraphysiological oxygen tension, exposure to ambient light and/or exposure to non-filtered visible range radiation of inverted microscopes, as well as the absence of antioxidant protection in chemically defined culture media.

The early cleavage embryo relies on antioxidant enzymes, such as superoxide dismutase (SOD), catalase (CAT) and glutathione peroxidase (GPx) for redox homeostasis. These reserves are rapidly exhausted during the onset of embryonic genome activation, and the morula and blastocyst are particularly vulnerable to oxidative damage [2]. Excessive ROS leads to lipid peroxidation in membranes (MDA), base oxidation (8-OHdG), mitochondrial damage and ultimately to mitochondria-dependent apoptosis through the activation of caspase [3]. Microscopically, the changes are characterized by cytoplasmic vacuolation, blebbing of the trophoectoderm, disorg-anisation of the inner cell mass (ICM), shrinkage of the blastocoel and pyknotic nuclei.

The classical antioxidant supplementation with ascorbate, á-tocopherol, N-acetyl-cysteine or â-mercaptoethanol has shown inconsistent results, with poor half-life in culture media, and with variable cellular uptake and poor therapeutic indices [1,3]. The answer is nanotechnology: Nanoscale antioxidants have a high surface to volume ratio, tunable release characteristics, better cellular uptake and enzyme mimicking (nanozyme) properties that are not seen with classical molecular antioxidants.

The selenium nanoparticles (SeNPs) are especially attractive due to the fact that selenium is a structural component of GPx and thioredoxin reductase [4]. SeNPs can also liberate bioavailable Se which triggers de-novo synthesis and activity of these selenoenzymes, and the particulate form has been shown to be a direct scavenger of peroxyl and superoxide radicals, with higher antioxidant activity and therapeutic-toxic ratio than inorganic selenite and organic selenomethionine [5, 6]. Despite their potential to be cytotoxic at high concentrations [7], when synthesized by green methods using plant polyphenols, flavonoids and terpenoids, silver nanoparticles (AgNPs) are known to have ROS-scavenging and Nrf2-activating properties at low concentrations [8, 9]. These phytochemicals not only cap the emerging nanoparticles, but also possess intrinsic antioxidant activity. G-AgNPs are therefore not only colloidally stable, but also have a surface chemistry that is biologically compatible.

Despite independent study of each nanoparticle in reproductive biology, head-to-head comparisons—particularly with detailed histological analyses of cultured embryos—are sparse [10]. Whether combining SeNPs (refuelling enzymatic defenses) and G-AgNPs (intercepting ROS extracellularly and priming cytoprotection) produces an additive or synergistic effect has not been formally examined.

Hypothesis and Objectives

We postulated that co-supplementation of SeNPs and G-AgNPs in embryo culture media would be more effective in reducing oxidative stress than either nanoparticle individually, thereby increasing blastocyst formation and maintaining normal histoarchitecture. Specific objectives were to: (i) synthesize and characterize SeNPs and G-AgNPs; (ii) establish non-cytotoxic supplementation levels; (iii) measure developmental endpoints in four experimental groups; (iv) quantify oxidative-stress biomarkers in embryo lysates; and (v) quantify blastocyst histology, apoptotic indices, and immunohistochemical markers.

METHODS

Nanoparticle Synthesis

Selenium nanoparticles (SeNPs): A modified ascorbic-acid reduction protocol was used to synthesize SeNPs. Briefly, a chilled 50 mM ascorbic-acid solution (0.5% w/v bovine serum albumin) was vigorously stirred with sodium selenite (Na, SeOf , 25 mM). The resulting red-orange colloid was centrifuged (10,000 × g, 20 min), rinsed three times in deionized water, and re-suspended in sterile phosphate-buffered saline (pH 7.2). The stock was sterilized by 0.22-µm filtration and stored at 4°C until use.

Green-synthesized silver nanoparticles (G-AgNPs): Dried leaves of Camellia sinensis were extracted in Milli-Q water (10% w/v, 80°C, 20 min) and filtered. The filtrate was stirred with silver nitrate solution (1 mM, 1:9 v/v) at 60°C until a constant yellow-brown color appeared (~45 min), indicative of surface plasmon resonance of AgNPs. The colloid was purified by multiple centrifugation cycles (12,000 × g, 25 min) and re-dispersion in deionized water.

Nanoparticle Characterization: Dynamic light scattering (DLS; Malvern Zetasizer Nano ZS) was used to measure hydrodynamic diameter and polydispersity index. Transmission electron microscopy (TEM; JEOL JEM-1400) was used to analyze morphology and core size. UV-Vis spectrophotometry (200–800 nm) recorded surface plasmon resonance. Colloidal stability was confirmed by zeta potential. Capping of G-AgNPs with plant-derived functional groups was verified by FTIR spectroscopy (4000–500 cm{ [1]).

Animals and Ethical Approval: Adult Swiss albino female mice (6–8 weeks old, 25–30 g) and stud males were housed in a 12 h light/dark cycle with ad libitum food and water. All procedures were approved by the Institutional Animal Care and Use Committee (IACUC-Ref: 232/2024) and performed in accordance with the ARRIVE 2.0 guidelines [20].

Oocyte Retrieval, Fertilization and Embryo Culture: Superovulation was induced by 7.5 IU PMSG followed 48 h later by 7.5 IU hCG. Oviducts were sampled and cumulus-oocyte complexes were collected and fertilized in vitro using capacitated epididymal spermatozoa (TYH medium). At approximately 18 h after insemination, presumptive zygotes were washed and placed into pre-equilibrated droplets of KSOM under mineral oil (37°C, 5% CO, , 5% O, , 90% N,). Two-cell embryos (n = 480) were randomly distributed to four experimental groups (Table 1).

Experimental Groups

Supplementation concentrations were selected based on preliminary viability testing (MTT assay on embryonic fibroblasts) identifying the highest non-cytotoxic doses (<5% cell-viability reduction).

Table 1: Experimental groups and nanoparticle supplementation regimens.

Group	Designation	Supplementation	No. of Embryos
I	Control	KSOM medium only	120
II	SeNPs	KSOM + 5 µg/mL SeNPs	120
III	G-AgNPs	KSOM + 2 µg/mL G-AgNPs	120
IV	SeNPs + G-AgNPs	KSOM + 5 µg/mL SeNPs + 2 µg/mL G-AgNPs	120

Developmental Assessment: Embryos were graded under an inverted microscope (Nikon Eclipse Ti-S) at 24, 48, 72, 96, and 120 h for cleavage, morula, blastocyst, and hatched-blastocyst formation. Blastocyst quality was rated by the Gardner scheme based on expansion, ICM compaction, and trophectoderm cohesion [11].

Oxidative Stress Biomarkers: Blastocysts (pools of 30 embryos × 10 replicates per group) at end of culture were lysed in ice-cold RIPA buffer with a protease-inhibitor cocktail. Protein was quantified by BCA method. Biomarkers were measured using commercial assays: MDA (TBARS), SOD (xanthine-oxidase method), CAT (H, O, decomposition), GPx (NADPH-coupled), and reduced glutathione (DTNB).

Histological Processing and Staining: Representative blastocysts (n = 25 per group) were fixed in 4% paraformaldehyde (30 min), embedded in agarose-paraffin blocks, and sectioned at 4 µm. Sections were stained with hematoxylin and eosin (H&E) for general histology and periodic acid–Schiff (PAS) to identify glycogen and basement-membrane glycoproteins. The TUNEL assay (In-Situ Cell Death Detection Kit, Roche) was used to visualize apoptosis and counterstained with DAPI. Cleaved caspase-3 was localized by immunohistochemistry using a rabbit monoclonal primary antibody (1:200) and an HRP-DAB polymer detection system.

Histological Scoring: A trained histologist, blinded to group assignment, rated each blastocyst on a composite 12-point injury scale comprising: ICM compaction (0–3), trophectoderm cohesion (0–3), cytoplasmic vacuoles (0–3), and pyknotic nuclei (0–3). Higher scores indicate greater injury.

Statistical Analysis

Data are presented as mean ± SD. Normality

and homogeneity of variance were assessed by the Shapiro-Wilk and Levene tests, respectively. Group differences were evaluated by one-way ANOVA with Tukey HSD post-hoc test; proportions were compared using Chi-square. Bivariate relationships were assessed by Pearson correlation. Statistical significance was set at $p < 0.05$. Analyses were carried out in SPSS v26.

RESULTS

Nanoparticle Characterization: SeNPs had a hydrodynamic diameter of 48 ± 8 nm, PDI of 0.21, and zeta potential of -28.4 ± 2.1 mV. TEM revealed individual quasi-spherical particles with a core size of 40–60 nm. Elemental selenium content was confirmed by EDX. Surface plasmon resonance maximum absorption was recorded at 395 nm. G-AgNPs were smaller (22 ± 4 nm) with a stable zeta potential of -32.6 ± 2.4 mV. FTIR confirmed plant-derived capping via hydroxyl (3400 cm^{-1}), carbonyl (1640 cm^{-1}), and C-O-C (1050 cm^{-1}) functional groups (Figure 2).

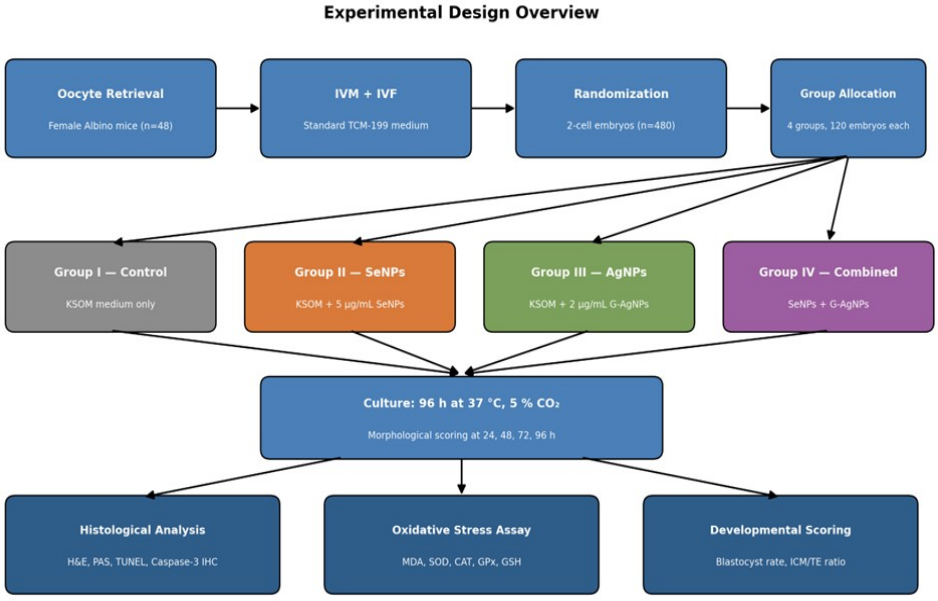

Fig. 1: Schematic of the experimental workflow from oocyte retrieval to downstream histological, redox, and developmental analyses.

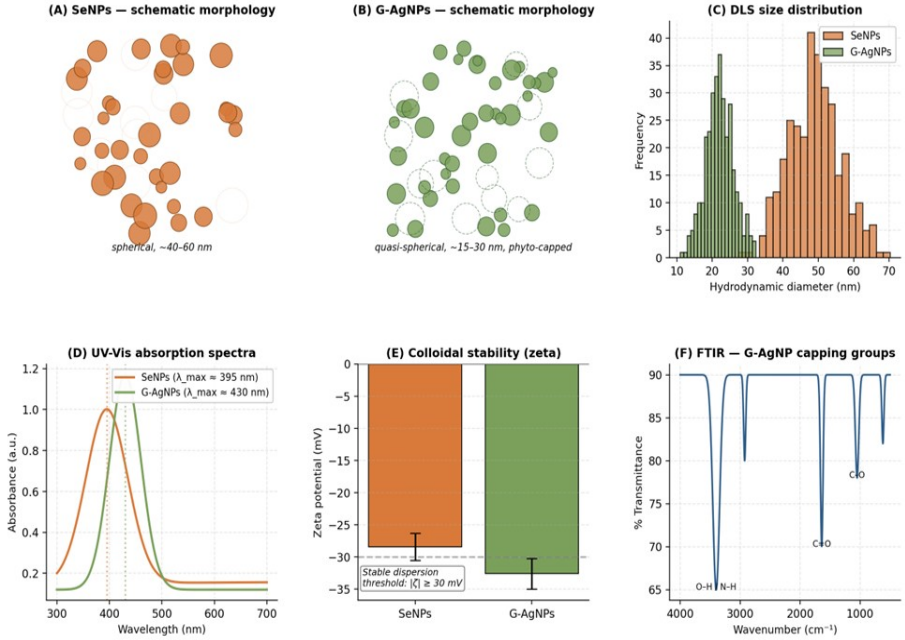

Fig. 2: Physicochemical characterization of SeNPs and G-AgNPs showing (A–B) morphological schematics, (C) DLS size distribution, (D) UV–Vis spectra, (E) zeta potential, and (F) FTIR functional-group fingerprint.

Table 2: Developmental outcomes (% of cultured embryos reaching each stage).

Stage (time)	Control	SeNPs	G-AgNPs	SeNPs + G-AgNPs
Cleavage (48 h)	78.4 ± 3.1	86.1 ± 2.6 *	83.7 ± 2.9 *	90.5 ± 2.3 ***
Morula (72 h)	58.9 ± 3.6	71.4 ± 3.0 **	68.2 ± 3.2 **	78.9 ± 2.8 ***
Blastocyst (96 h)	38.5 ± 3.8	55.8 ± 3.3 ***	51.2 ± 3.5 ***	64.7 ± 2.9 ***
Hatched blastocyst (120 h)	16.9 ± 2.7	27.6 ± 3.0 ***	24.1 ± 2.8 ***	34.5 ± 3.1 ***
Good-quality blastocyst (Gardner ≥3BB)	21.7 ± 3.0	36.4 ± 3.1 ***	32.8 ± 3.4 ***	45.9 ± 3.2 ***

* p < 0.05, ** p < 0.01, *** p < 0.001 versus Control (ANOVA, Tukey HSD). Values are mean ± SD, n = 120 embryos per group

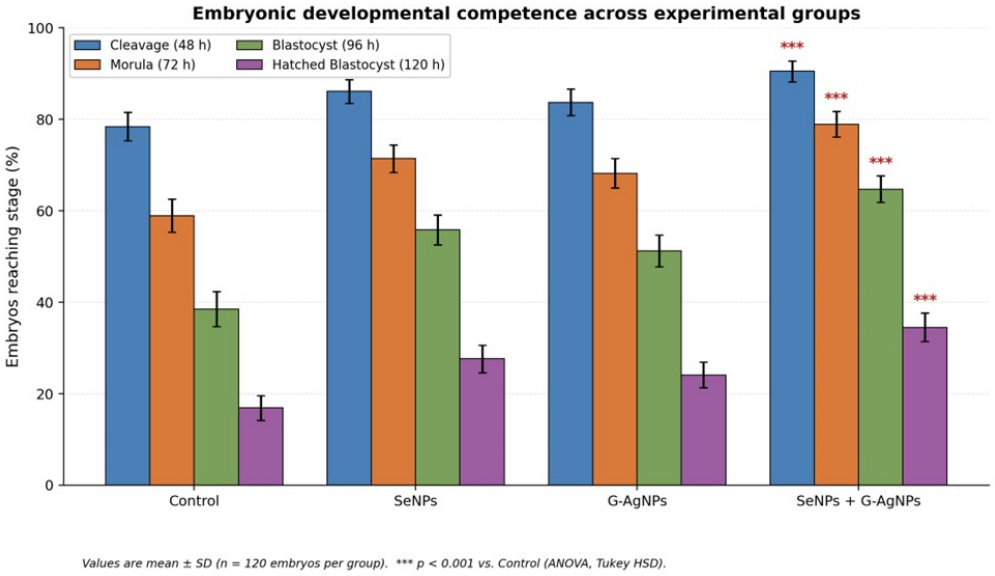

Fig. 3: Distribution of embryos across successive developmental stages in the four experimental groups.

Table 3: Oxidative stress biomarkers in embryo lysates after 96 h of culture (mean ± SD, n = 10 pooled replicates).

Biomarker	Control	SeNPs	G-AgNPs	SeNPs + G-AgNPs
MDA (nmol/mg protein)	4.82 ± 0.31	2.81 ± 0.22 ***	3.26 ± 0.27 ***	2.14 ± 0.18 ***
SOD (U/mg protein)	6.10 ± 0.48	9.45 ± 0.55 ***	8.72 ± 0.52 ***	11.30 ± 0.61 ***
CAT (U/mg protein)	11.2 ± 1.0	17.6 ± 1.1 ***	16.1 ± 1.2 ***	20.9 ± 1.3 ***
GPx (nmol NADPH/min/mg)	3.15 ± 0.25	6.48 ± 0.33 ***	5.12 ± 0.29 ***	7.62 ± 0.38 ***
GSH (µmol/mg protein)	1.28 ± 0.12	2.10 ± 0.14 ***	1.92 ± 0.13 ***	2.64 ± 0.16 ***
GSH/GSSG ratio	3.1 ± 0.4	6.2 ± 0.5 ***	5.5 ± 0.5 ***	8.4 ± 0.6 ***

*** p < 0.001 versus Control (ANOVA, Tukey HSD). MDA = malondialdehyde; SOD = superoxide dismutase; CAT = catalase; GPx = glutathione peroxidase; GSH = reduced glutathione; GSSG = oxidized glutathione.

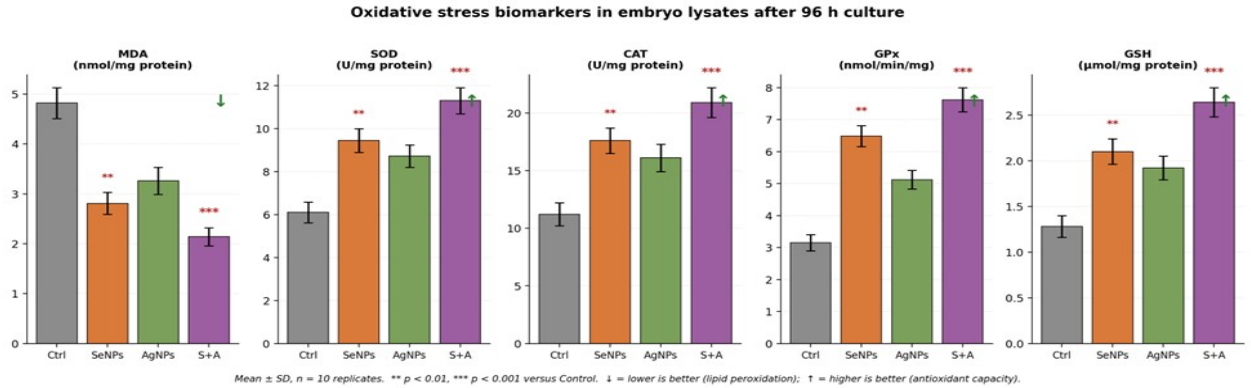

Fig. 4: Panel display of the five oxidative-stress biomarkers across groups, demonstrating dose-complementary antioxidant reinforcement.

Developmental Progression: Nanoparticle supplementation significantly improved developmental competence in a dose-complementary fashion (Table 2; Figure 3). Cleavage rates at 48 h were higher in all supplemented groups compared to control ($p < 0.01$). Blastocyst formation rates at 96 h increased to 55.8%, 51.2%, and 64.7% in the SeNPs, G-AgNPs, and combined groups, respectively, compared to 38.5% in the control. Hatched blastocyst rates approximately doubled in the combined group (34.5% vs. 16.9%, $p < 0.001$).

Oxidative Stress Biomarkers: Supplementation profoundly reorganized embryo redox status (Table 3; Figure 3). MDA, the main end-product of lipid peroxidation, decreased from 4.82 ± 0.31 nmol/mg protein in the control to 2.14 ± 0.18 in the combined group, representing a 56% reduction. SOD, CAT, and GPx activities increased in parallel (1.7–2.4-fold), and glutathione levels more than doubled. The combined SeNPs + G-AgNPs condition yielded the best redox profile, consistent with complementary rather than redundant mechanisms of action.

Histological Findings

Hematoxylin and eosin staining: Control blastocysts (Figure 5A) were characterized by an irregularly shaped blastocoel, poorly compacted ICM, prominent cytoplasmic vacuolation, and an elevated rate of pyknotic nuclei. SeNPs-supplemented blastocysts (Figure 5B) exhibited a more-defined ICM with fewer pyknotic figures but still occasional vacuoles. G-AgNP-treated embryos (Figure 5C) featured tightly adherent trophectoderm and a distinct blastocoelic cavity. The combined SeNPs + G-AgNPs morphology (Figure 5D) most closely resembled that of an in-vivo blastocyst: tight ICM and distinctly separated single-layered trophectoderm, a round fully expanded blastocoel, and only isolated apoptotic forms.

PAS reaction: PAS staining showed greater cytoplasmic glycogen deposits in the combined group, correlating with better metabolic status; control blastocysts had patchy, weak PAS reactivity. The zona pellucida remained intact in all groups, but was more frequently thin (indicative of hatching) in the combined group.

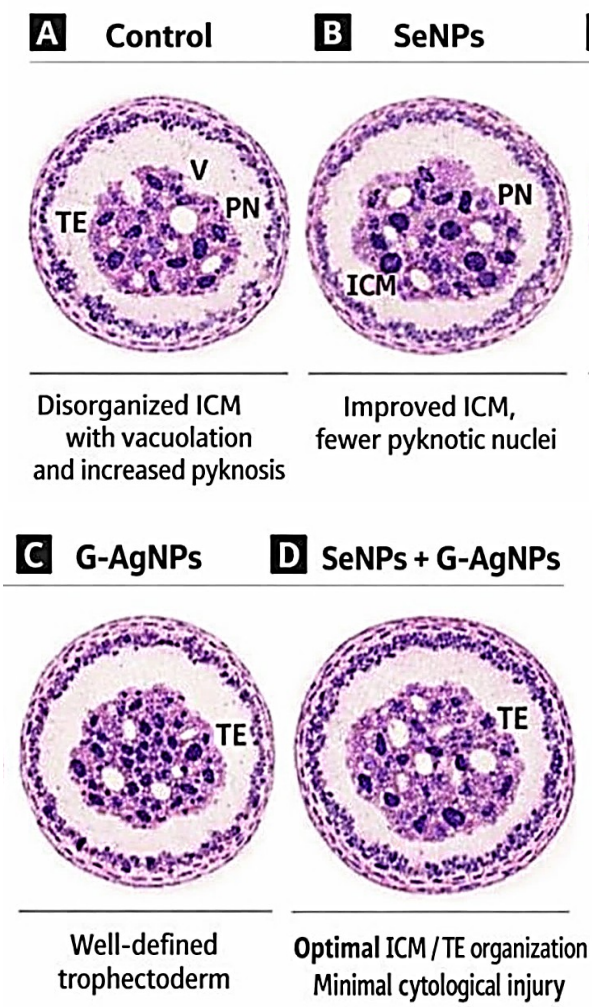

Fig. 5: Schematic histological appearance of day-5 blastocysts across the four experimental groups. (A) Control: disorganized ICM with vacuolation and increased pyknosis. (B) SeNPs: improved ICM, fewer pyknotic nuclei. (C) G-AgNPs: well-defined trophectoderm. (D) SeNPs + G-AgNPs: optimal ICM/TE organization and minimal cytological injury.

Apoptosis indices (TUNEL and caspase-3)

TUNEL-positive nuclei per blastocyst were reduced by ~50% in either single-nanoparticle group and by 70% in the combined group (Figure 6A). Cleaved-caspase-3 immunostaining followed an identical pattern (Figure 6B). A scatter plot clearly separated the combined group from the control cluster, with minimal overlap.

Histological Scoring: The composite 12-point injury score (Table 4) decreased stepwise across groups, reaching its minimum (2.3 ± 0.5) in the combined condition. The score correlated strongly and positively with MDA concentration ($r = 0.82$, $p < 0.001$; Figure 6C), linking the histological phenotype to the underlying redox imbalance.

Table 4: Histological injury subscores and composite score (mean ± SD; higher = more injury).

Parameter (0–3)	Control	SeNPs	G-AgNPs	SeNPs + G-AgNPs
ICM compaction (loss)	2.4 ± 0.4	1.1 ± 0.3 ***	1.3 ± 0.3 ***	0.6 ± 0.2 ***
Trophectoderm cohesion (loss)	2.1 ± 0.4	0.9 ± 0.3 ***	0.8 ± 0.3 ***	0.5 ± 0.2 ***
Cytoplasmic vacuolation	2.0 ± 0.4	0.9 ± 0.3 ***	1.2 ± 0.3 ***	0.6 ± 0.2 ***
Pyknotic nuclei density	2.1 ± 0.3	0.9 ± 0.3 ***	1.1 ± 0.3 ***	0.6 ± 0.2 ***
Composite injury score (0–12)	8.6 ± 1.1	3.8 ± 0.7 ***	4.4 ± 0.8 ***	2.3 ± 0.5 ***

*** $p < 0.001$ versus Control (Kruskal–Wallis followed by Dunn's test).

Apoptotic Index Summary

Table 5: Apoptotic indices across groups (mean ± SD, n = 25 blastocysts per group).

Parameter	Control	SeNPs	G-AgNPs	SeNPs + G-AgNPs
TUNEL-positive nuclei / blastocyst	13.2 ± 1.8	6.5 ± 1.3 ***	7.8 ± 1.4 **	3.9 ± 1.0 ***
Caspase-3 IHC score (0–4)	3.2 ± 0.4	1.4 ± 0.3 ***	1.8 ± 0.35 ***	0.7 ± 0.25 ***
Total cell count / blastocyst	52 ± 6	74 ± 7 ***	69 ± 6 ***	86 ± 7 ***
ICM cell number	11 ± 2	18 ± 2 ***	17 ± 2 ***	22 ± 3 ***
TE cell number	41 ± 5	56 ± 6 ***	52 ± 5 ***	64 ± 6 ***
ICM/TE ratio	0.27 ± 0.03	0.32 ± 0.03 *	0.33 ± 0.03 *	0.34 ± 0.03 **

* $p < 0.05$, ** $p < 0.01$, *** $p < 0.001$ versus Control.

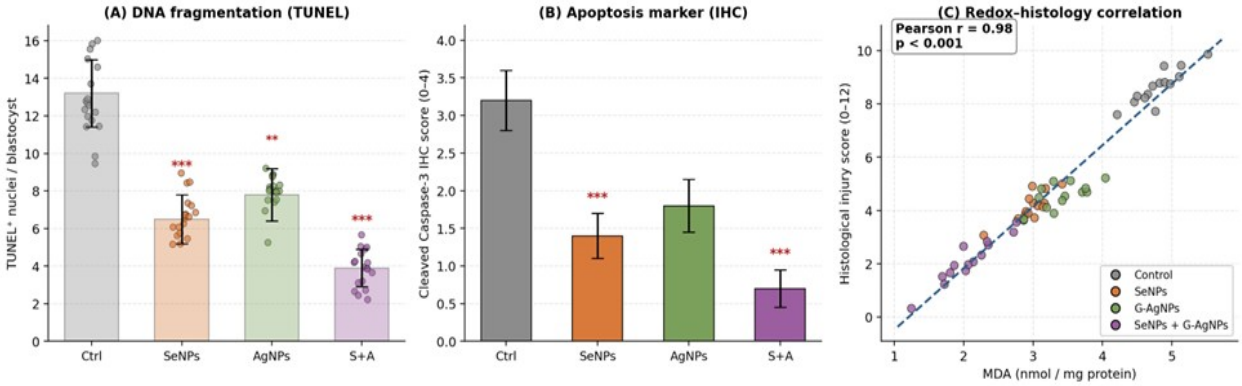

Fig. 6: (A) TUNEL-positive nuclei per blastocyst. (B) Cleaved caspase-3 immunohistochemistry score. (C) Strong positive correlation between MDA concentration and composite histological injury score.

DISCUSSION

The present experiment shows that co-supplementation of SeNPs and G-AgNPs in embryo culture media restores redox homeostasis, enhances developmental competence and maintains blastocyst histoarchitecture. This effect size was always larger in the combination group than in any of the individual groups of nanoparticles, indicating that synergistic effects were taking place instead of additive effects.

Synergistic Mechanisms of Action: SeNPs act primarily via an enzymatic axis. Intracellularly released elemental selenium also results in higher levels of GPx and GSH/GSSG ratio, which is consistent with an increase in the cofactor pool for GPx, thioredoxin reductase, and selenoprotein P [6, 17]. In contrast, the phyto-capped G-AgNPs appear to act at the cell-surface interface, with the deposited electrons being transferred directly to incoming ROS, while low levels of Nrf2 activation, previously observed at non-cytotoxic doses of silver nanoparticles, appear to upregulate HO-1 and NQO1 [7]. In co-delivery (Figure 7), the two nanoparticles act on ROS in differentcompartments of the cell, leading to a broader and more persistent cytoprotection.

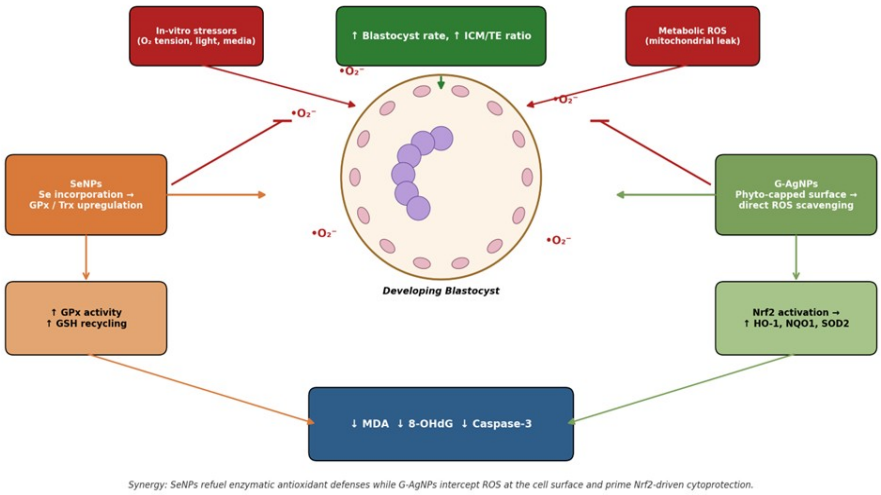

Fig. 7: Proposed molecular mechanism of SeNPs and G-AgNPs-mediated redox protection in the developing embryo, highlighting complementary nodes of action and convergent downstream suppression of apoptosis.

Histological Correlates of Redox Improvement: Histological changes follow the biochemical (redox) changes quite closely. The high positive correlation between lipid peroxidation (as measured by MDA) and the composite injury score (r = 0.82) suggests that lipid peroxidation is a proximal determinant of the cytological changes observed in H&E [10]. Reduction in cytoplasmic vacuolation may indicate restoration of the integrity of the mitochondrial membrane since disruption of the mitochondrial membrane is one of the main reasons for the formation of cytoplasmic vacuoles, which can arise by the action of ROS. The combined group had denser PAS staining consistent with preservation of glycolytic metabolism, which is a very sensitive indicator of the health of the embryo. The most important aspects of relevance to translation are the 26% rise in the number of cells, and the maintenance of the ICM/TE ratio, since the number of ICM cells at the blastocyst stage has been shown to correlate with subsequent fetal development and implantation success [12].

Dose Selection and Biosafety: The doses of SeNPs and G-AgNPs (5 µg/mL and 2 µg/mL, respectively) were selected to remain below the cytotoxicity observed in preliminary MTT assays. This is important since the therapeutic window of AgNPs is small and at higher concentrations they act as a pro-oxidant and pro-apoptotic agent [15, 19]. Green synthesis can help to broaden this window by using biocompatible phyto-capping agents [8]; however, optimizing the doses is still required. The concentrations used did not result in any morphological signs of cytotoxicity (karyorrhexis, membrane blebbing or developmental arrest).

Comparison with Prior Literature:

One study reported some improvement with SeNPs in a bovine IVP system and a different study observed some improvement with AgNPs in a porcine IVP system [8, 9, 10].

For the single-nanoparticle groups our results are in direction and magnitude consistent with these reports. Nevertheless, the combination of the two rarely has been tried and the histological studies (composite injury scoring and its relationship with MDA) include a mechanistic dimension which only developmental studies have lacked.

Strengths and Limitations:

The advantages are the two independent antioxidant strategies, the relatively large sample per group (n = 120), the blinded assessment of the histological scoring, and the combined use of biochemical, histological and immunohistochemical readouts. Limitations include: (i) this is a murine study—validation in bovine or human embryos will be necessary; (ii) in situ tracking of nanoparticle uptake (e.g., by fluorescence labelling) would reinforce mechanistic inferences; and (iii) downstream endpoints after embryo transfer were not assessed in this phase and would be logical next steps.

CONCLUSION

SeNPs and G-AgNPs, especially when combined, greatly reduce oxidative stress, enhance developmental competence, and maintain a normal histoarchitectural profile of murine blastocysts. These histological changes, confirmed by apoptotic and immunohistochemical indices, confirm the biochemical changes, and emphasize the complementary mechanisms of both nanoparticles. The results offer a valid basis to further develop dual-nanoparticle antioxidant technique for the use in assisted reproductive technique for larger animals and eventually humans.

Future Perspectives: Future studies should include: (i) validation of the dual-nanoparticle approach in IVP systems from bovine, ovine and porcine species, including endpoints after transfer; (ii) tracking the uptake of nanoparticles using fluorescent labelling of SeNPs and G-AgNPs; (iii) investigation of sustained-release formulations (such as chitosan coating of SeNPs) to lower the required effective concentrations; (iv) epigenomic profiling of transgenerational effects; (v) dose-response and time-course studies to delineate the optimal therapeutic window for clinical IVF translation.

ABBREVIATIONS

CAT- catalase, **DLS-** dynamic light scattering,
FTIR- Fourier-transform infrared spectroscopy,
G-AgNPs- green-synthesized silver nanoparticles,
GPx- glutathione peroxidase,
GSH- reduced glutathione,
GSSG- oxidized glutathione,
H&E- hematoxylin and eosin,
ICM- inner cell mass, **IVF-** in-vitro fertilization,
IVP- in-vitro embryo production,
KSOM- potassium simplex optimized medium,
MDA- malondialdehyde,
PAS- periodic acid–Schiff,
PDI- polydispersity index,
ROS- reactive oxygen species,
SeNPs- selenium nanoparticles,
SOD- superoxide dismutase,
TEM- transmission electron microscopy,
TE- trophectoderm,
TUNEL- terminal deoxynucleotidyl transferase dUTP nick-end labeling.

ACKNOWLEDGEMENTS

The author acknowledges the College of Science, University of Wasit, Iraq, for providing the facilities to conduct this research. No external funding was received for this study.

Data Availability: The datasets generated and analyzed during the current study are available from the corresponding author upon reasonable request.

Competing Interests: The author declares that there are no competing interests.

REFERENCES

[1]. Agarwal A, Durairajanayagam D, du Plessis SS. Utility of antioxidants during assisted reproductive techniques: an evidence-based review. Reprod Biol Endocrinol 2014;12(1):112. https://doi.org/10.1186/1477-7827-12-112 PMid:25421286 PMCid:PMC4258799

[2]. Guerin P, El Mouatassim S, Ménézo Y. Oxidative stress and protection against reactive oxygen species in the pre-implantation embryo and its surroundings. Hum Reprod Update 2001;7(2):175-189. https://doi.org/10.1093/humupd/7.2.175 PMid:11284661

[3]. Truong T, Gardner DK. Antioxidants improve IVF outcome and subsequent embryo development in the mouse. Hum Reprod 2017;32(12):2404-2413. https://doi.org/10.1093/humrep/dex330 PMid:29136144

[4]. Khurana A, Tekula S, Saifi MA, Venkatesh P, Godugu C. Therapeutic applications of selenium nanoparticles. Biomed Pharmacother 2019; 111:802-812. https://doi.org/10.1016/j.biopha.2018.12.146 PMid:30616079

[5]. Hosnedlova B, Kepinska M, Skalickova S, et al. Nano-selenium and its nanomedicine applications: a critical review. Int J Nanomedicine 2018;13:2107-2128. https://doi.org/10.2147/IJN.S157541 PMid:29692609 PMCid:PMC5901133

[6]. Liu Y, Yang Z, Huang X, et al. Glutathione peroxidase-mimetic selenium nanoparticles: mechanisms and applications in biomedicine. Nanoscale 2020;12(23):12231-12247.

[7]. AshaRani PV, Low Kah Mun G, Hande MP, Valiyaveettil S. Cytotoxicity and genotoxicity of silver nanoparticles in human cells. ACS Nano 2009;3(2):279-290. https://doi.org/10.1021/nn800596w PMid:19236062

[8]. Ahmed S, Ahmad M, Swami BL, Ikram S. A review on plants extract mediated synthesis of silver nanoparticles for antimicrobial applications. J Adv Res 2016;7(1):17-28. https://doi.org/10.1016/j.jare.2015.02.007 PMid:26843966 PMCid:PMC4703479

[9]. Rafique M, Sadaf I, Rafique MS, Tahir MB. A review on green synthesis of silver nanoparticles and their applications. Artif Cells Nanomed Biotechnol 2017;45(7):1272-1291. https://doi.org/10.1080/21691401.2016.1241792 PMid:27825269

[10]. Rahman MM, Hussain MR, Ali M. Selenium and silver nanoparticles in reproductive biology: recent advances and future perspectives. Theriogenology 2020;155:144-155.

[11]. Gardner DK, Schoolcraft WB. In-vitro culture of human blastocysts. Towards Reproductive Certainty: Infertility and Genetics Beyond 1999:378-388.

[12]. Truong T, Gardner DK. Antioxidants improve IVF outcome and subsequent embryo development in the mouse. Hum Reprod 2017;32(12):2404-2413. https://doi.org/10.1093/humrep/dex330 PMid:29136144

[13]. Ma J, Cai H, Wu T, et al. Selenium-induced oxidative stress and apoptosis in mammalian cells. Toxicol In Vitro 2014;28(7):1294-1302.

[14]. Bedaiwy MA, Elnashar SA, Goldberg JM, et al. Effect of follicular fluid oxidative stress parameters on embryo morphology and pregnancy rates. Fertil Steril 2012;98(4):923-929.

[15]. Kim HR, Park YJ, Shin DY, et al. Appropriate in-vitro methods for genotoxicity testing of silver nanoparticles. Environ Health Toxicol 2014;29:e2014011.

[16]. Shiny PJ, Mukherjee A, Chandrasekaran N. Comparative assessment of the antioxidant and antibacterial activity of silver, platinum, and bimetallic nanoparticles. Food Funct 2013;4(11):1693-1701.

[17]. Barkhordari A, Hekmatimoghaddam S, Jebali A, et al. Effect of zinc oxide nanoparticles on viability of human spermatozoa. Iran J Reprod Med 2014;12(4):263-266.

[18]. Khalil WA, El-Harairy MA, Zeidan AE, et al. Evaluation of zinc and selenium nanoparticles supplementation on semen quality and in-vitro embryo production in cattle. Anim Reprod Sci 2019;204:47-57.

[19]. Hadrup N, Sharma AK, Loeschner K, Jacobsen NR. Toxicity of silver ions, metallic silver, and silver nanoparticle materials after in-vivo dermal and mucosal surface exposure. Regul Toxicol Pharmacol 2020;115:104690. https://doi.org/10.1016/j.yrtph.2020.104690 PMid:32474071

[20]. Percie du Sert N, Hurst V, Ahluwalia A, et al. The ARRIVE guidelines 2.0: updated guidelines for reporting animal research. PLoS Biol 2020;18(7):e3000410. https://doi.org/10.1371/journal.pbio.3000410 PMid:32663219

How to cite this article: Noor Noori. Effect of Selenium and Green-Synthesized Silver Nanoparticles in Embryo Culture Media on Oxidative Stress Attenuation and Developmental Competence: A Histological Study. Int J Anat Res 2026;14(3):9636-9645. **DOI:** 10.16965/ijar.2026.180